HHS Public Access

Author manuscript

J Biomater Sci Polym Ed. Author manuscript; available in PMC 2017 June 01.

Published in final edited form as:

J Biomater Sci Polym Ed. 2016 June ; 27(8): 721–742. doi:10.1080/09205063.2016.1155881.

Temporal and spatial distribution of macrophage phenotype markers in the foreign body response to glutaraldehyde-crosslinked gelatin hydrogels

Tony Yu[1,¶], **Wenbo Wang**[2,¶], **Sina Nassiri**[1], **Thomas Kwan**[3], **Chau Dang**[1], **Wei Liu**[2], and **Kara L. Spiller**[1,*]

[1]School of Biomedical Engineering, Science, and Health Systems, Drexel University, Philadelphia, PA, USA

[2]Shanghai Key Tissue Engineering Laboratory, Shanghai Jiao Tong University, 639 Zhizaoju Road, Shanghai, China

[3]Institute of Science and Technology in Medicine, Keele University, Stoke-on-Trent, United Kingdom

Abstract

In recent years, macrophage phenotype has emerged as an important determinant of the success or failure of implanted polymeric biomaterials. However, it is not well understood how changes in biomaterials properties affect the foreign body response or macrophage behavior. Because failed attempts at biomaterial degradation by macrophages have been linked to frustrated phagocytosis, a defining feature of the foreign body response, we hypothesized that increased hydrogel crosslinking density (and decreased degradability) would exacerbate the foreign body response. Gelatin hydrogels were crosslinked with glutaraldehyde (0.05%, 0.1%, and 0.3%) and implanted subcutaneously in C57BL/6 mice over the course of 3 weeks. Histological and immunohistochemical analysis was used to characterize fibrous capsule formation and the temporal and spatial distribution of macrophage phenotype markers. Interestingly, changes in hydrogel crosslinking did not affect the thickness of the fibrous capsule surrounding the hydrogels, expression of the pan-macrophage marker F480, expression of three macrophage phenotype markers (iNOS, Arg1, CD163), or expression of the myofibroblast marker aSMA. With respect to temporal changes, the level of expression of the M1 marker (iNOS) remained relatively constant throughout the study, while the M2 markers Arg1 and CD163 increased over time. Expression of these M2 markers was highly correlated with fibrous capsule thickness. Differences in spatial distribution of staining also were noted, with the strongest staining for iNOS at the hydrogel surface and increasing expression of the myofibroblast marker aSMA toward the outer edge of the fibrous capsule. These results confirm previous reports that macrophages in the foreign body response exhibit characteristics of both M1 and M2 phenotypes. Understanding the effects (or lack

[*]Corresponding author: Kara L. Spiller, PhD, Drexel University, School of Biomedical Engineering, Science, and Health Systems, 3141 Chestnut St., Bossone 718, Philadelphia, PA 19104, ; Email: spiller@drexel.edu (K.L.S)

[¶]Co-First Authors

present address: Shrewsbury and Telford Hospitals NHS Trust

7. Disclosure statement The authors declare no direct financial interest or benefit from this research.

of effects) of biomaterial properties on the foreign body response and macrophage phenotype may aid in the rational design of biomaterials to integrate with surrounding tissue.

1. Introduction

Biomaterials face an inflammatory environment upon implantation, which often leads to medical device failures. The injury caused by biomaterial implantation triggers the inflammatory response, characterized by the recruitment of neutrophils, followed by monocytes that differentiate into macrophages. Macrophages attempt to degrade the material, fuse into foreign body giant cells, and encapsulate it in fibrous tissue, isolating it from the rest of the body [1]. This foreign body response (FBR) and the formation of the fibrous capsule limit the function of many medical devices, especially diffusion-dependent devices, sensors, and engineered tissues that are intended to integrate with the surrounding tissue. While several attempts have been made to inhibit formation of the fibrous capsule, including making the surface of the biomaterial more hydrophilic or more biomimetic [2–4], a completely successful strategy has not yet been realized.

Macrophages play an essential role in the FBR to implanted biomaterials. Macrophages can rapidly shift their behavior from pro-inflammatory to anti-inflammatory. These very different activation states are commonly referred to as M1 and M2, respectively, although it is now understood that two categories are not sufficient to characterize macrophages, and that they often exhibit characteristics associated with multiple activation states [5, 6]. In normal wound healing, the phenotype of the macrophage population is largely M1 at early times after injury, peaking at 1–5 days and then decreasing [7, 8]. The M1 phenotype is associated with the release of pro-inflammatory cytokines and clearance of bacteria and tissue debris [9], and initiation of angiogenesis [10]. As wound healing progresses, the macrophage population shifts from primarily M1 to primarily M2, which gradually accumulate until they peak around 7–14 days, at least in mice [7, 8]. The M2 phenotype is associated with the resolution of inflammation, and involves phagocytosis of apoptotic cells [9] as well as extracellular matrix synthesis and tissue remodeling [11]. If the M1-to-M2 transition is disrupted, wounds suffer from chronic inflammation [12, 13].

Both M1 and M2 macrophages have been linked to the FBR. In some studies, higher levels of M2 macrophages surrounding implanted biomaterials relative to M1 macrophages has been associated with more constructive remodeling [14, 15]. As a result, strategies to actively promote M2 activation of macrophages have emerged [16–18]. In support of this idea, ultra low-fouling hydrogels that successfully avoided fibrous encapsulation in a subcutaneous implantation model were surrounded by higher numbers of M2 markers than M1 markers [2]. On the other hand, M2 macrophages are known to contribute to the FBR. For example, the M2-stimulating cytokine interleukin-4 (IL4) stimulates foreign body giant cell formation *in vitro* [19] and fibrous capsule formation *in vivo* [20], and inhibition of M2 activity via blocking macrophage mannose receptor (MMR/CD206) inhibits fibrous capsule formation *in vivo* [21]. Moreover, M2 macrophages are known to contribute to fibrosis in numerous pathological situations [22, 23]. Recently, Mooney *et al.* used a transgenic mouse model with fluorescent macrophages to show that macrophages in the fibrous capsule

surrounding cubes of boiled egg whites, a model foreign body, exhibited traits characteristic of both M1 and M2 macrophages [24] and even expressed high levels of the myofibroblast marker alpha-smooth muscle actin (aSMA) [25]. Thus, it appears likely that both M1 and M2 macrophages, including hybrid phenotypes in between, contribute to fibrous encapsulation of biomaterials [26].

The effects of biomaterial properties on the behavior of macrophages and the FBR are not well understood. For example, only a few studies have investigated the complex relationship between hydrogel mechanical properties and macrophage behavior *in vivo*. One study showed that a decrease in poly(ethylene glycol) (PEG)-based hydrogel stiffness (and increase in swelling ratio) resulted in a decrease in the thickness of the fibrous capsule following implantation in C57BL/6 mice for 28 days, concomitant with a decrease in inflammatory (i.e., M1) gene expression by macrophages [27]. In contrast, another study found that different degradation profiles, and therefore different elastic modulus profiles, of PEG-based hydrogels did not affect macrophage phenotype or the FBR in a similar mouse model [28].

In comparison to non-crosslinked gelatin hydrogels, crosslinking with relatively low concentrations of glutaraldehyde has been shown to increase inflammatory cell infiltration following subcutaneous implantation in Sprague-Dawley rats, but a stainless steel cage was required to hold the gelatin hydrogels, which are not stable for more than a day *in vitro* or *in vivo* [29]. While no differences were noted in the inflammatory response to hydrogels crosslinked with 0.01% or 0.1% glutaraldehyde, the presence of the stainless steel cage would undoubtedly have affected the FBR, obscuring interpretation of the results. Thus, the goal of this study was to further characterize the effects of glutaraldehyde crosslinking of gelatin hydrogels on the FBR, using concentrations of glutaraldehyde that are substantially lower than those used in the preparation of collagen-based materials for clinical use, including bioprosthetic heart valves [30, 31] and wound dressings [32]. The secondary goal of this work was to evaluate changes in macrophage phenotype over time to further understand how they contribute to the formation of the fibrous capsule in the FBR.

Because a failure to successfully degrade biomaterials by macrophages has been linked to “frustrated phagocytosis” that precedes fibrous encapsulation of biomaterials [1], we hypothesized that increased hydrogel crosslinking density, and therefore decreased degradation, would exacerbate the FBR and affect macrophage behavior. To test this hypothesis, we characterized the response of macrophages in the FBR to gelatin hydrogels that were crosslinked to different extents with glutaraldehyde. The hydrogels were implanted subcutaneously in mice and analyzed via immunohistochemistry for commonly employed markers of macrophage phenotypes and of myofibroblasts at early, middle, and late time points over the course of 3 weeks.

2. Materials and Methods

2.1. Preparation of crosslinked gelatin hydrogels

Gelatin solution (10wt%, Sigma Aldrich, Type B bovine skin) was prepared in phosphate buffered saline (PBS) and sterilized by boiling. 8 mL of the gelatin solution was transferred

into 100mm × 15mm dishes and allowed to cool to room temperature. The dishes were incubated at 4°C until gelation was complete. Then, a 5mm biopsy punch was used to punch the gelatin into cylindrical disks. The gelatin hydrogels were then crosslinked via immersion in sterile-filtered solutions of 0%, 0.05%, 0.1%, and 0.3% glutaraldehyde (Sigma Aldrich) on a shaker overnight. The hydrogels were then washed 4 times in PBS for 15 minutes. Finally, the hydrogels were immersed in sterile-filtered 0.1M glycine (Sigma Aldrich) solution in a shaker overnight to neutralize any residual glutaraldehyde. The hydrogels were washed an additional two times in sterile PBS for 15 minutes each. The hydrogels were then held under UV light in a biosafety cabinet (typical radiation 40μW/cm^2) for at least 2 hours to ensure sterilization [33].

2.2. Hydrogel characterization

2.2.1. Mechanical properties—Characterization of the hydrogels was performed following sterilization so that the reported crosslinking densities would not be affected by any UV-induced crosslinking. Hydrogels were mechanically tested in compression tests using a Bose Electroforce 3100 Test Instrument. Using a caliper, the dimensions of the hydrogels were measured. The hydrogels were compressed to 30% strain at a rate of 0.333% strain per second. The slope of the initial linear region of the stress-strain curve was considered the Young's modulus. Only the curve between 5–7% strain was used to calculate the slope in order to reduce variability.

2.2.2. Crosslinking density—The crosslinking density of each hydrogel was calculated using the modified Flory Rehner equation [34]:

$$\frac{-\left[ln\left(1-v_p\right)+v_p+\chi*v_p^2\right]}{\rho*V_1*\left(v_p^{\frac{1}{3}}-\frac{v_p}{2}\right)}=\varepsilon \quad (1)$$

where ε is the crosslinking density, v_p is the polymer volume fraction, χ is the polymer-solvent interaction parameter, ρ is the density of the polymer, and V_1 is the molar volume of water, the solvent. v_p was calculated using the following equations:

$$v_p=\frac{V}{V_c} \quad (2)$$

$$V=\frac{w_p}{\rho} \quad (3)$$

where V is the volume of the gelatin hydrogel, V_c is the volume of the swollen hydrogel, w_p is the weight of the hydrogel, and ρ is the density of gelatin. χ was obtained from the literature [34].

2.2.3. Swelling ratio—The swelling ratio of the hydrogels was calculated by the following equation [34]:

$$swelling\ Ratio = \frac{w_s - w_d}{w_d} \quad (4)$$

where w_s is the swollen weight and w_d is the dry weight. The swollen weight was calculated by measuring the mass of the hydrogels after allowing them to reach equilibrium by swelling in PBS overnight. The hydrogels were then allowed to dry at room temperature in order to measure the dry weight.

2.2.4. Degradation profile—Enzymatic degradation of the hydrogels was monitored over the course of one week in collagenase solution (from *Clostridium histolyticum*, 5μg/ml, Sigma Aldrich), using a concentration that is similar to that used in a study that found good correlation between *in vitro* and *in vivo* degradation profiles of gelatin-based hydrogels [35]. The mass of each hydrogel was recorded every 24 hours after blotting dry on a paper towel to determine the percent mass loss over time.

2.3. Murine subcutaneous implantation model

All animal experimental protocols were approved by an Institutional Review Committee of the Shanghai Jiao Tong University School of Medicine. C57BL/6 6–8 week old male mice were anesthetized with choral hydrate and shaved prior to surgery. This mouse strain was chosen because its macrophages have been extensively characterized in comparison to human macrophages [36, 37], and because it has been used for many studies of the FBR. Three incisions were made with scissors in the dorsum of each mouse in order to implant the three hydrogels crosslinked at 0.05%, 0.1, and 0.3%. Because non-crosslinked hydrogels dissolve rapidly *in vitro* and *in vivo* [29], they were not included in this study. Pockets were made under the skin with blunt forceps and one sample from each crosslinking concentration was implanted into each mouse for 3 days, 10 days, or 3 weeks (n=6 mice per time point). The first incision was made at the top of the back body, right below the neck. The second incision was made on the left side of the back body, next to the left back legs. The third and final incision was made on the right side of the back body, next to the right back legs. After hydrogel implantation, the sites were sutured with three sutures. The mice were monitored daily for any signs of infections or abnormalities. Previous studies have indicated that the subcutaneous implantation surgery does not result in a persistent inflammatory response, and no fibrous capsule forms, so a sham surgery was not included.

2.4. Sample explantation and histological preparation

At each time point, the mice were euthanized by cervical dislocation and the hydrogels were explanted. Each hydrogel was surrounded by a fibrous capsule and attached to the skin. The hydrogels and the surrounding tissues were immediately fixed in 4% paraformaldehyde for 24 hours. Then, the hydrogels were washed for 8 hours in PBS. The samples then underwent dehydration in an ethanol series followed by xylene replacement, embedding in paraffin, and sectioning to a thickness of 5 μm. To ensure uniform staining conditions across groups, one section from each group of crosslinking concentrations were sectioned onto the same slide for each time point.

2.5. Histological analysis

Tissue sections were heated at 70°C for 45 minutes to melt the paraffin wax, then deparaffinized in 100% CitriSolv (Sigma Aldrich) for 5 minutes. The sections were then rehydrated in a reverse ethanol series before staining. To visualize the fibrous capsule, the samples were stained with Masson's trichrome and counterstained with hematoxylin according to the manufacturer's instructions (Sigma Aldrich).

2.6. Immunohistochemistry (IHC)

IHC was employed to detect macrophage phenotype marker expression in serial sections. Numerous previous studies have shown that the fibrous capsule consists almost entirely of macrophages that exhibit characteristics of both M1 and M2 macrophages [2, 10, 24, 38]. Thus, our intention was to expand on these works that have counted individual cells staining positively for each marker by evaluating changes in the *intensity* of expression of these markers in the hybrid phenotypes over time, which is important for characterization of macrophage phenotype [10] but extremely difficult to do with immunofluorescent analysis that would have allowed single cell analysis. Indeed, the density of macrophages in the fibrous capsule make accurate analysis of single cells extremely difficult when using DAB staining, even at high magnification (Fig. S1).

After deparaffinization of the samples, antigen retrieval was performed by immersion in 10mM sodium citrate (Sigma Aldrich) and heating until just before boiling for 20 minutes. The samples were cooled to room temperature and washed with running tap water. Endogenous peroxidase was blocked with BLOXALL solution of the ImmPress Excel staining kit (Vector Laboratories). The samples were then washed in the buffer 2x for 5 minutes each. Nonspecific binding was blocked with 2.5% normal horse serum in PBS for 20 minutes. The primary antibodies monoclonal rat-anti-mouse F4/80 (eBiosciences catalog no. 14-4801-81, dilution 1:50 1% BSA), polyclonal rabbit anti-mouse iNOS (Abcam, catalog no. ab15323, dilution 1:50 1% BSA), polyclonal goat anti-mouse Arg1 (Santa Cruz Biotechnology, catalog no. sc-18354, dilution 1:100 in 1% BSA), polyclonal rabbit anti-mouse CD163 (Santa Cruz Biotechnology, catalog no. sc-33560, dilution 1:100 in 1% BSA), or polyclonal rabbit anti-mouse α-SMA (Abcam, catalog no. ab15734, dilution 1:50 in 1% BSA) were added to the samples and incubated overnight at 4°C. The samples were washed twice in buffer solution for 5 minutes each. The ImmPress Excel secondary antibody (horse anti-rabbit or horse anti-goat as necessary) was then added to the samples and incubated for 45 minutes. The samples were washed three times in buffer solution for 5 minutes each and then staining was visualized with 3,3'-diaminobenzidine (DAB) (1:10 dilution). Each sample was exposed to 100 μL of DAB for 1 minute and was subjected to the same concentration, amount, and exposure time to DAB as it can directly affect the intensity of staining. Care was taken to ensure that the conditions used to develop color with DAB within each antibody group were consistent between all samples, because DAB staining can vary with the amount of time exposed to the samples, concentration, and even day-to-day variations. Positive and negative controls were used in each batch of staining. Samples incubated without primary antibody were used as the negative control, and sections of mouse spleen were used as the positive control. Isotype controls were also used to confirm minimal non-specific staining (Fig. S2).

2.7. Imaging and quantification

All stained samples were imaged in bright field via an EVOS optical microscope. The thickness of the fibrous capsule from Masson's trichrome staining was quantified at the hydrogel-tissue interface of both the left and right sides of the hydrogel using ImageJ. A line was drawn from the edges of the fibrous capsule, and the length (in pixels) was measured. The value in units of pixels was converted to μm based on the magnification of the image.

The mean intensity of the IHC staining was quantified rather than cell count of positively stained cells, following previous studies that showed via flow cytometry that mean intensity is a more accurate indicator of phenotype [10]. Low magnification images were used to ensure that the maximum amount of tissue was analyzed after confirming that trends in expression levels were not different between low and high magnification images. The intensity of expression of each marker was quantified in ImageJ using the Plot Profile tool. A line was drawn from the hydrogel surface through the fibrous capsule to a fixed distance determined by the quantification of the fibrous capsule using Masson's trichrome staining. The Plot Profile tool measures the pixel intensity values along the line and provides the intensity values in a table. These data were used to determine the average intensity and the spatial distribution of staining intensity from the inside (closer to the hydrogel) to the outside (closer to the tissue) of the fibrous capsule. When quantifying intensity in RGB images, darker pixels have lower values than lighter pixels. Therefore, the level of expression of each marker was calculated by subtracting the values from the max value (255) and then dividing by the maximum value to result in a normalized value of intensity. The intensity of each surface marker was evaluated at both the muscle- and skin-facing sides of the hydrogel. Student's t-test indicated there was no statistical difference between the locations measured. Thus, the values of expression of each marker on both sides were averaged for further analysis. Negative controls were included for each IHC experiment as a baseline for comparison and to differentiate between background staining and real staining.

2.8. Statistical analysis

Data are reported as mean ± standard deviation. Statistical analysis was performed in GraphPad Prism 5.0. A one- or two-way ANOVA with Tukey's post hoc multiple comparison analysis was performed as required to determine statistical significance among the different crosslinking densities and the different time points. For analysis of IHC results, a p-value of less than 0.01 was considered significant. Correlation analyses were conducted to determine any relationships between the macrophage phenotype and the fibrous capsule thickness. The Pearson's correlation coefficient was calculated at two-tailed 95% confidence interval.

3. Results

3.1. Hydrogel characterization

As expected, the Young's moduli of the hydrogels increased with increasing crosslinking concentration of glutaraldehyde (Fig. S3a). Similarly, increasing concentration of glutaraldehyde also increased crosslinking density (Fig. S3b), and decreased equilibrium swelling ratio (Fig. S3c). The rate at which the hydrogels degraded in collagenase solution

decreased with increasing crosslinking, as shown by decreasing mass over time (Fig. S3d). From day 7 to day 13, the percent weight loss of the hydrogels in each group was significantly different from each other ($p<0.05$, Fig. S3d).

3.2. Histological and IHC analysis

The thickness of the fibrous capsule following subcutaneous implantation in mice increased over time for all samples (two-way ANOVA, $p<0.01$), but no differences were observed with respect to degree of crosslinking at any time point (Fig. 1).

IHC analysis was performed to quantify intensity of staining of surface markers associated with all macrophages (F4/80), the M1 phenotype (iNOS), the M2 phenotype (Arg1 and CD163), and myofibroblasts (aSMA). No differences were observed in mean F4/80 intensity between different crosslinking concentrations or over time (Fig. 2). Slight decreases in iNOS staining intensity were observed from 3 to 21 days, but this decrease was only significant for hydrogels crosslinked with 0.3% glutaraldehyde (Fig. 3). In contrast, expression of the M2 markers Arg1 (Fig. 4) and CD163 (Fig. 5) increased over time for all groups of hydrogels ($p<0.01$, two way ANOVA). No differences were observed in average intensity of staining for aSMA, a myofibroblast marker (Fig. 6). In summary, no statistically significant differences were observed in staining for any of the markers as a result of different crosslinking concentrations ($p>0.05$, two way ANOVA).

3.3. Spatial distribution of staining

The spatial distribution of macrophage phenotype markers in the fibrous capsule was determined for a representative group of samples, the hydrogels crosslinked with 0.3% glutaraldehyde after 3 weeks of implantation (Fig. 7). Both F4/80 and iNOS were more strongly expressed at the interior of the fibrous capsule where it interfaced with the hydrogels implants, regardless of crosslinking concentration or time (Fig. 7a–b). The M2 marker Arg1 stained evenly throughout the fibrous capsule (Fig. 7c) while CD163 slightly decreased toward the outer edge (Fig. 7d). Staining of α-SMA increased towards the outer edge of the fibrous capsule (Fig. 7e). The M2/M1 ratio, defined as the ratio of iNOS expression to the average of Arg1 and CD163 expression, increased slightly from the hydrogel surface to the outer edge (Fig. 7f).

3.4. Correlation analyses

Correlation analyses were performed to determine the relationships between fibrous capsule thickness and macrophage phenotype markers across all hydrogel groups and time points (Fig. S4). Expression of F480 and iNOS were not correlated with thickness of the fibrous capsule. In contrast, there was a strong positive relationship between fibrous capsule thickness and both M2 surface markers, Arg1 and CD163, with Pearson correlation coefficients of 0.851 and 0.943, respectively. Unexpectedly, there was a strong negative correlation between the expression of α-SMA and the fibrous capsule thickness ($R = -0.932$). Finally, there was a positive correlation between the M2/M1 ratio, defined as the average of the expression levels of Arg1 and CD163 divided by the expression of iNOS, with a Pearson correlation coefficient of 0.823.

4. Discussion

In recent years, landmark studies have shown that macrophage phenotype is a critical indicator of biomaterial success or failure [14, 39]. However, the effects of hydrogel properties on macrophage behavior are not well understood. In this study, our hypothesis that increased hydrogel crosslinking would exacerbate the FBR and affect macrophage behavior was rejected, at least for the first 21 days of the FBR and the range of glutaraldehyde concentrations tested in this study. Nonetheless, this work does add to the growing body of literature that suggests that both M1 and M2 macrophages contribute to formation of the fibrous capsule in the FBR.

Glutaraldehyde crosslinking of biomaterials was first introduced in the late 1960s to reduce immunogenicity of allogeneic or xenogeneic implants such as heart valves [40]. Crosslinking of protein-based biomaterials with glutaraldehyde occurs through covalent bonds that form between the aldehyde groups of glutaraldehyde and primary amine groups in the protein backbone of gelatin. Thus, the foreign molecule glutaraldehyde is directly incorporated into the crosslinked material, which may trigger inflammation. Indeed, glutaraldehyde-crosslinked biomaterials (albeit with much higher concentrations than those used here) were shown to induce M1-related gene expression in macrophages *in vitro* [41].

Many studies have been performed over the years to evaluate the FBR to glutaraldehyde-crosslinked biomaterials [42–45]. While the concentrations of glutaraldehyde used in the present work were substantially lower than those used in the preparation of clinically utilized bioprosthetic heart valves [30] and wound dressings [32], it is likely that the lowest concentration of glutaraldehyde studied here was sufficient to induce as much inflammation as the highest concentration. At least two studies previously showed that 0.1% glutaraldehyde crosslinking of collagen or gelatin implants was sufficient to induce the FBR in rats, with no further increase in response to 0.3% glutaraldehyde, but these samples were only evaluated qualitatively at 30 days following implantation and macrophage behavior was not assessed [29, 46]. Interestingly, glutaraldehyde crosslinking of porous collagen scaffolds was shown to cause scaffold vascularization in mice, rats, and guinea pigs, compared to non-crosslinked scaffolds that were encapsulated in fibrous capsule [10, 46]. In one study it was shown that this vascularization was concomitant with infiltration of macrophages exhibiting mixed M1/M2 phenotypes [10]. Taken together, these results suggest that there is still a need to better understand how scaffold crosslinking and macrophage behavior interact to affect biomaterial outcome.

Besides the incorporation of inflammatory molecules, the effects of glutaraldehyde crosslinking on the FBR may be due to changes in physical properties of the hydrogels. Increasing hydrogel crosslinking density causes an increase in elastic modulus, which has been reported to increase the severity of the FBR in C57BL/6 mice to PEG-based hydrogels with similar elastic moduli and swelling ratios to the hydrogels tested here [27]. Although we did not find an increase in the FBR to hydrogels with increasing moduli, differences in the inflammatory potential of the materials may explain the apparently conflicting results.

Increasing crosslinking of gelatin hydrogels also decreases their ability to be degraded. As in our study, others have also reported a lack of influence of crosslinking density or degradation profile of both oligo(PEG-fumarate) and chitosan hydrogels on the FBR in rabbits and rats [47, 48], although macrophage phenotype was not evaluated in these studies. Moreover, Safranski *et al*. showed that degradation rate of PEG-based hydrogels did not affect the thickness of the fibrous capsule or staining intensity for iNOS or Arg1 after 8 weeks of subcutaneous implantation in mice [28], in agreement with our results. Although these studies are not exhaustive, separate groups have now reported the counterintuitive finding that degradation rate does not have a significant effect on macrophage phenotype or on the FBR to crosslinked hydrogels made from both synthetic and natural polymers. Taken together, these results suggest that it may be possible to tailor hydrogel degradation profile without affecting the FBR.

M1 macrophages are often associated with inflammation and the FBR, while M2 macrophages are typically associated with healing and constructive remodeling [15, 39, 49]. The present study shows a clear correlation between M2 marker staining and fibrous capsule thickness. In agreement with our study, a study of PEG-based hydrogels also found constant levels of gene expression of iNOS and increasing gene expression of Arg1 in the fibrous capsule over 4 weeks in C57BL/6 mice [50]. Interestingly, this study also reported increasing expression of the pro-inflammatory cytokine interleukin-1-beta (IL1b) over time, which was also found in another study of macrophage gene expression in fibrous capsule formation in the MacGreen mouse, a C57BL/6-CBA strain with fluorescent macrophages [24], suggesting a role for the M1-associated cytokine in the FBR. This latter study also reported increasing levels of an M2 marker, *Chi313*, which is in agreement with our study in which we found increasing levels of the M2 markers Arg1 and CD163. Thus, although we and others found a lack of correlation between iNOS (M1) expression and fibrous capsule thickness, it is likely that macrophages with a predominantly M1 phenotype still contribute to the foreign body response, since persistent levels of M1 macrophages were observed over time, whereas they typically diminish over time in normal wound healing [7, 51]. In addition, both M1 and M2 macrophages secrete factors implicated in the formation of the fibrous capsule, including M1-secreted tumor necrosis factor-α (TNFα) [52] as well as M2-secreted platelet derived growth factor (PDGF) and transforming growth factor-β (TGF-β) [10, 20, 53]. In addition, recent studies that isolated macrophages from fibrous capsules noted that they exhibited characteristics of both M1 and M2 macrophages, and even resembled fibroblasts [24, 25]. Moreover, the addition of both M1- and M2-promoting stimuli (tumor necrosis factor alpha and IL13, respectively) to macrophages *in vitro* causes substantial increases in their secretion of the pro-fibrotic factor transforming growth factor-beta compared to the effects of either stimulus individually [54]. Taken together, these results suggest that either 1) both M1 and M2 macrophages cooperate to promote progression of the FBR, or 2) hybrid M1–M2 macrophages typify the FBR. Single cell analyses will be required to determine which of these explanations is more likely.

Previous studies have reported that the M2/M1 ratio was indicative of healing in spinal cord injury [55], chronic wounds [13], and inflammatory renal disease [56], and of constructive remodeling of implanted surgical mesh biomaterials [15]. In these studies, fibrous capsule formation did not occur. On the other hand, in studies where the M2/M1 ratio was assessed

within the fibrous capsule surrounding biomaterials, a higher M2/M1 ratio was associated with the fibrous capsule, as in the present study [50, 57, 58]. Taken together, these results suggest that the fibrous encapsulation of biomaterials can be considered a wound healing response that fails to resolve, a theory that has been previously proposed [1, 59].

Another interesting finding of this study was that F4/80 (the pan-macrophage marker) and iNOS (the M1 marker) stained more strongly in the interior of the fibrous capsule (at the hydrogel interface), while Arg1 and CD163 (M2 markers) stained uniformly throughout the fibrous capsule. It is not surprising that macrophages in direct contact with the glutaraldehyde-crosslinked hydrogels were more inflamed (i.e. M1). Moreover, since newly arriving macrophages did not interface directly with the foreign body, but rather with the collagen of the fibrous capsule, it makes sense that they would be less inflamed. Interestingly, aSMA, the myofibroblast marker, increased in expression level from the interior to the exterior of the fibrous capsule. Macrophages in the fibrous capsule have been shown to stain for aSMA [24, 25], and monocytes are known to differentiate into fibroblast-like cells called fibrocytes [60], so it is not possible to definitively distinguish between macrophages and fibroblasts. Future studies are required to delineate the roles of and interactions between macrophages and fibroblasts in the FBR.

A major limitation of this study was the use of only a few macrophage phenotype markers to characterize their behavior. It is well known that macrophages exist on a broad and diverse spectrum of phenotypes, which includes hybrid phenotypes, and a few surface markers are insufficient to fully characterize their complex behavior. It is important to note that the macrophages of the fibrous capsule appear to exhibit hybrid M1/M2 phenotypes and should not be labeled as one or the other [24, 26]. Moreover, dual labeling to evaluate co-expression of markers may have been more informative. In addition, a more detailed biological analysis of the numerous secreted factors that are likely important in mediating the FBR would be beneficial to further understand the behavior of macrophages with shifting phenotypes. Another limitation is that this study was limited to 3 weeks of subcutaneous implantation; it is possible that changes in macrophage behavior as a function of crosslinking could occur at later time points, when the hydrogels are closer to full degradation. Finally, the findings of this study may be different in different animal models. We chose this mouse model because its macrophages have been thoroughly characterized in comparison to human macrophages [36] and because many mouse models of the foreign body response utilize this strain. However, C57BL/6 mice are considered Th1-biased because of higher levels of Th1 cytokine production in the spleen [61]. Macrophages from C57BL/6 mice and those from Th2-biased mice such as Balb/c mice differ with respect to arginine catabolism, resulting in differences in macrophage behavior even though cytokine-induced expression of Arg1 and Nos2 are not different on either the gene or protein level between macrophages from the two strains [62]. How the differences in arginine transport affect the response of macrophages to foreign objects such as biomaterials is an important question that deserves further scrutiny.

Certain other limitations to this study may prevent extension of the results described herein to other classes of biomaterials. Gelatin hydrogels were chosen for this study because gelatin is a commonly used enzymatically degradable naturally-derived polymer [63, 64], and because the properties of gelatin hydrogels, including crosslinking density and degradation

profile, can be easily controlled via chemical crosslinking with glutaraldehyde [29, 65, 66]. However, increasing crosslinking also increases mechanical properties and decreases degradability, obscuring interpretation of the effects of these properties on the foreign body response. In addition, different biomaterials have different chemical and physical properties that would further alter the behavior of macrophages and the FBR from normal wound healing. Another limitation of using gelatin as a model biomaterial is that like other animal-derived polymers, it may be immunogenic, but these effects were not studied here. Finally, the FBR to the hydrogels was only studied in a subcutaneous implantation model and not in orthotopic locations where stress from blood flow and other mechanical stimuli may influence a change in the polarization of macrophage phenotypes. While some studies have shown that there is no difference in the fibrous capsule formation between subcutaneous and cranial implantation [47], others have found that site of implantation can have a major effect [67, 68]. Nonetheless, the subcutaneous implantation model does allow controlled and reproducible studies of the inflammatory response [69].

5. Conclusion

This study showed that glutaraldehyde-crosslinked gelatin hydrogels elicit a strong foreign body response when implanted subcutaneously in mice, characterized by encapsulation in fibrous tissue, persistent levels of the M1 macrophage marker iNOS, and increasing levels of M2 macrophage markers Arg1 and CD163. Interestingly, the extent of the FBR or macrophage response was not affected by the degree of hydrogel crosslinking or degradation. This study emphasizes the complexity of the role of macrophage polarization in biomaterial outcome and suggests that further studies are required to fully elucidate the effects of biomaterial properties on macrophage polarization and the FBR.

Supplementary Material

Refer to Web version on PubMed Central for supplementary material.

Acknowledgements

The authors gratefully acknowledge technical assistance from Emily Lurier, Nathan Tessema Ersumo, Dev Patel and Valerie Tutwiler from Drexel University, Chen Lulu, Zhu Yueqian, and Lian Jie from Shanghai Jiao Tong University, and the Kimmel Cancer Center Consortium of Thomas Jefferson University. T.Y. is grateful for a Whitaker International Undergraduate Scholarship Program. This work was supported in part by a Burroughs Wellcome Fund Collaborative Research Travel Grant to K.L.S (Grant Number 1012766) and an NHLBI R01 grant to KLS (Grant number HL130037-01).

8. References

1. Anderson JM, Rodriguez A, Chang DT. Foreign body reaction to biomaterials. Semin Immunol. 2008; 20(2):86–100. [PubMed: 18162407]
2. Zhang L, Cao Z, Bai T, Carr L, Ella-Menye JR, Irvin C, et al. Zwitterionic hydrogels implanted in mice resist the foreign-body reaction. Nat Biotechnol. 2013; 31(6):553–6. [PubMed: 23666011]
3. Schulz MC, Korn P, Stadlinger B, Range U, Moller S, Becher J, et al. Coating with artificial matrices from collagen and sulfated hyaluronan influences the osseointegration of dental implants. J Mater Sci Mater Med. 2014; 25(1):247–58. [PubMed: 24113890]

4. Rammelt S, Illert T, Bierbaum S, Scharnweber D, Zwipp H, Schneiders W. Coating of titanium implants with collagen, RGD peptide and chondroitin sulfate. Biomaterials. 2006; 27(32):5561–71. [PubMed: 16879866]
5. Mosser DM, Edwards JP. Exploring the full spectrum of macrophage activation. Nat Rev Immunol. 2008; 8(12):958–69. [PubMed: 19029990]
6. Xue J, Schmidt SV, Sander J, Draffehn A, Krebs W, Quester I, et al. Transcriptome-based network analysis reveals a spectrum model of human macrophage activation. Immunity. 2014; 40(2):274–88. [PubMed: 24530056]
7. Arnold L, Henry A, Poron F, Baba-Amer Y, van Rooijen N, Plonquet A, et al. Inflammatory monocytes recruited after skeletal muscle injury switch into antiinflammatory macrophages to support myogenesis. J Exp Med. 2007; 204(5):1057–69. [PubMed: 17485518]
8. Troidl C, Mollmann H, Nef H, Masseli F, Voss S, Szardien S, et al. Classically and alternatively activated macrophages contribute to tissue remodelling after myocardial infarction. J Cell Mol Med. 2009; 13(9B):3485–96. [PubMed: 19228260]
9. Brown KL, Poon GF, Birkenhead D, Pena OM, Falsafi R, Dahlgren C, et al. Host defense peptide LL-37 selectively reduces proinflammatory macrophage responses. J Immunol. 2011; 186(9):5497–505. [PubMed: 21441450]
10. Spiller KL, Anfang RR, Spiller KJ, Ng J, Nakazawa KR, Daulton JW, et al. The role of macrophage phenotype in vascularization of tissue engineering scaffolds. Biomaterials. 2014; 35(15):4477–88. [PubMed: 24589361]
11. Gratchev A, Kzhyshkowska J, Utikal J, Goerdt S. Interleukin-4 and dexamethasone counterregulate extracellular matrix remodelling and phagocytosis in type-2 macrophages. Scand J Immunol. 2005; 61(1):10–7. [PubMed: 15644118]
12. Sindrilaru A, Peters T, Wieschalka S, Baican C, Baican A, Peter H, et al. An unrestrained proinflammatory M1 macrophage population induced by iron impairs wound healing in humans and mice. J Clin Invest. 2011; 121(3):985–97. [PubMed: 21317534]
13. Nassiri S, Zakeri I, Weingarten MS, Spiller KL. Relative Expression of Proinflammatory and Antiinflammatory Genes Reveals Differences between Healing and Nonhealing Human Chronic Diabetic Foot Ulcers. J Invest Dermatol. 2015; 135(6):1700–3. [PubMed: 25647438]
14. Brown BN, Valentin JE, Stewart-Akers AM, McCabe GP, Badylak SF. Macrophage phenotype and remodeling outcomes in response to biologic scaffolds with and without a cellular component. Biomaterials. 2009; 30(8):1482–91. [PubMed: 19121538]
15. Brown BN, Londono R, Tottey S, Zhang L, Kukla KA, Wolf MT, et al. Macrophage phenotype as a predictor of constructive remodeling following the implantation of biologically derived surgical mesh materials. Acta Biomater. 2012; 8(3):978–87. [PubMed: 22166681]
16. Mokarram N, Merchant A, Mukhatyar V, Patel G, Bellamkonda RV. Effect of modulating macrophage phenotype on peripheral nerve repair. Biomaterials. 2012; 33(34):8793–801. [PubMed: 22979988]
17. Boehler RM, Kuo R, Shin S, Goodman AG, Pilecki MA, Gower RM, et al. Lentivirus delivery of IL-10 to promote and sustain macrophage polarization towards an anti-inflammatory phenotype. Biotechnol Bioeng. 2014; 111(6):1210–21. [PubMed: 24375008]
18. Kou PM, Babensee JE. Macrophage and dendritic cell phenotypic diversity in the context of biomaterials. J Biomed Mater Res A. 2011; 96(1):239–60. [PubMed: 21105173]
19. Milde R, Ritter J, Tennent GA, Loesch A, Martinez FO, Gordon S, et al. Multinucleated Giant Cells Are Specialized for Complement-Mediated Phagocytosis and Large Target Destruction. Cell Rep. 2015; 13(9):1937–48. [PubMed: 26628365]
20. Kao WJ, McNally AK, Hiltner A, Anderson JM. Role for interleukin-4 in foreign-body giant cell formation on a poly(etherurethane urea) in vivo. J Biomed Mater Res. 1995; 29(10):1267–75. [PubMed: 8557729]
21. McNally AK, DeFife KM, Anderson JM. Interleukin-4-induced macrophage fusion is prevented by inhibitors of mannose receptor activity. Am J Pathol. 1996; 149(3):975–85. [PubMed: 8780401]
22. Murthy S, Larson-Casey JL, Ryan AJ, He C, Kobzik L, Carter AB. Alternative activation of macrophages and pulmonary fibrosis are modulated by scavenger receptor, macrophage receptor with collagenous structure. FASEB J. 2015

23. Furukawa S, Moriyama M, Tanaka A, Maehara T, Tsuboi H, Iizuka M, et al. Preferential M2 macrophages contribute to fibrosis in IgG4-related dacryoadenitis and sialoadenitis, so-called Mikulicz's disease. Clin Immunol. 2015; 156(1):9–18. [PubMed: 25450336]
24. Mooney JE, Summers KM, Gongora M, Grimmond SM, Campbell JH, Hume DA, et al. Transcriptional switching in macrophages associated with the peritoneal foreign body response. Immunol Cell Biol. 2014; 92(6):518–26. [PubMed: 24638066]
25. Mooney JE, Rolfe BE, Osborne GW, Sester DP, van Rooijen N, Campbell GR, et al. Cellular plasticity of inflammatory myeloid cells in the peritoneal foreign body response. Am J Pathol. 2010; 176(1):369–80. [PubMed: 20008135]
26. Moore LB, Kyriakides TR. Molecular Characterization of Macrophage-Biomaterial Interactions. Adv Exp Med Biol. 2015; 865:109–22. [PubMed: 26306446]
27. Blakney AK, Swartzlander MD, Bryant SJ. The effects of substrate stiffness on the in vitro activation of macrophages and in vivo host response to poly(ethylene glycol)-based hydrogels. J Biomed Mater Res A. 2012; 100(6):1375–86. [PubMed: 22407522]
28. Safranski DL, Weiss D, Clark JB, Caspersen BS, Taylor WR, Gall K. Effect of poly(ethylene glycol) diacrylate concentration on network properties and in vivo response of poly(beta-amino ester) networks. J Biomed Mater Res A. 2011; 96(2):320–9. [PubMed: 21171151]
29. Stevens KR, Einerson NJ, Burmania JA, Kao WJ. In vivo biocompatibility of gelatin-based hydrogels and interpenetrating networks. J Biomater Sci Polym Ed. 2002; 13(12):1353–66. [PubMed: 12555901]
30. Manji RA, Zhu LF, Nijjar NK, Rayner DC, Korbutt GS, Churchill TA, et al. Glutaraldehyde-fixed bioprosthetic heart valve conduits calcify and fail from xenograft rejection. Circulation. 2006; 114(4):318–27. [PubMed: 16831988]
31. Christian AJ, Lin H, Alferiev IS, Connolly JM, Ferrari G, Hazen SL, et al. The susceptibility of bioprosthetic heart valve leaflets to oxidation. Biomaterials. 2014; 35(7):2097–102. [PubMed: 24360721]
32. Matttern, RH.; Pierschbacher, MD.; Cahn, F.; Tschopp, JF.; Maloney, TI.; inventors. Integra Lifesciences Corporation, assignee. Collagen/glycosaminoglycan matrix stable to sterilizing by electron beam radiation. 2005.
33. Zhao L, Mei S, Wang W, Chu PK, Wu Z, Zhang Y. The role of sterilization in the cytocompatibility of titania nanotubes. Biomaterials. 2010; 31(8):2055–63. [PubMed: 20022370]
34. Akin H, Hasirci N. Preparation and characterization of crosslinked gelatin microspheres. Journal of Applied Polymer Science. 1995; 58(1):95–100.
35. Chen YC, Lin RZ, Qi H, Yang Y, Bae H, Melero-Martin JM, et al. Functional Human Vascular Network Generated in Photocrosslinkable Gelatin Methacrylate Hydrogels. Adv Funct Mater. 2012; 22(10):2027–39. [PubMed: 22907987]
36. Schroder K, Irvine KM, Taylor MS, Bokil NJ, Le Cao KA, Masterman KA, et al. Conservation and divergence in Toll-like receptor 4-regulated gene expression in primary human versus mouse macrophages. Proc Natl Acad Sci U S A. 2012; 109(16):E944–53. [PubMed: 22451944]
37. Martinez FO, Helming L, Milde R, Varin A, Melgert BN, Draijer C, et al. Genetic programs expressed in resting and IL-4 alternatively activated mouse and human macrophages: similarities and differences. Blood. 2013; 121(9):e57–69. [PubMed: 23293084]
38. Madden LR, Mortisen DJ, Sussman EM, Dupras SK, Fugate JA, Cuy JL, et al. Proangiogenic scaffolds as functional templates for cardiac tissue engineering. Proc Natl Acad Sci U S A. 2010; 107(34):15211–6. [PubMed: 20696917]
39. Badylak SF, Valentin JE, Ravindra AK, McCabe GP, Stewart-Akers AM. Macrophage phenotype as a determinant of biologic scaffold remodeling. Tissue Eng Part A. 2008; 14(11):1835–42. [PubMed: 18950271]
40. Nimni ME, Cheung D, Strates B, Kodama M, Sheikh K. Chemically modified collagen: a natural biomaterial for tissue replacement. J Biomed Mater Res. 1987; 21:741–71. [PubMed: 3036880]
41. Witherel CE, Graney PL, Freytes DO, Weingarten MS, Spiller KL. Response of human macrophages to wound matrices in vitro. Wound Repair and Regeneration. 2016 in press.

42. Ye Q, Harmsen M, van Luyn MJ, Bank RA. The relationship between collagen scaffold cross-linking agents and neutrophils in the foreign body reaction. Biomaterials. 2010; 31:9192–201. [PubMed: 20828809]
43. van Wachem PB, van Luyn MJ, Olde Damink LH, Dijkstra PJ, Feijen J, Nieuwenhuis P. Biocompatibility and tissue regenerating capacity of crosslinked dermal sheep collagen. J Biomed Mater Res. 1994; 28(3):353–63. [PubMed: 8077250]
44. Speer DP, Chvapil M, Eskelson CD, Ulreich J. Biological effects of residual glutaraldehyde in glutaraldehyde-tanned collagen biomaterials. Journal of Biomedical Materials Research. 1980; 14:753–64. [PubMed: 6820019]
45. Delgado LM, Bayon Y, Pandit A, Zeugolis DI. To cross-link or not to cross-link? Cross-linking associated foreign body response of collagen-based devices. Tissue Eng Part B Rev. 2015; 21(3): 298–313. [PubMed: 25517923]
46. McPherson JM, Sawamura S, Armstrong R. An examination of the biologic response to injectable, glutaraldehyde cross-linked collagen implants. J Biomed Mater Res. 1986; 20(1):93–107. [PubMed: 3949825]
47. Shin H, Quinten Ruhe P, Mikos AG, Jansen JA. In vivo bone and soft tissue response to injectable, biodegradable oligo(poly(ethylene glycol) fumarate) hydrogels. Biomaterials. 2003; 24(19):3201–11. [PubMed: 12763447]
48. Azab AK, Doviner V, Orkin B, Kleinstern J, Srebnik M, Nissan A, et al. Biocompatibility evaluation of crosslinked chitosan hydrogels after subcutaneous and intraperitoneal implantation in the rat. J Biomed Mater Res A. 2007; 83(2):414–22. [PubMed: 17455216]
49. Ratner BD. Healing with medical implants: The body battles back. Sci Transl Med. 2015; 7(272): 272fs4.
50. Lynn AD, Blakney AK, Kyriakides TR, Bryant SJ. Temporal progression of the host response to implanted poly(ethylene glycol)-based hydrogels. J Biomed Mater Res A. 2011; 96(4):621–31. [PubMed: 21268236]
51. Troidl C, Jung G, Troidl K, Hoffmann J, Mollmann H, Nef H, et al. The temporal and spatial distribution of macrophage subpopulations during arteriogenesis. Curr Vasc Pharmacol. 2013; 11(1):5–12. [PubMed: 23391417]
52. Verjee LS, Verhoekx JS, Chan JK, Krausgruber T, Nicolaidou V, Izadi D, et al. Unraveling the signaling pathways promoting fibrosis in Dupuytren's disease reveals TNF as a therapeutic target. Proc Natl Acad Sci U S A. 2013; 110(10):E928–37. [PubMed: 23431165]
53. Baker DW, Tsai YT, Weng H, Tang L. Alternative strategies to manipulate fibrocyte involvement in the fibrotic tissue response: pharmacokinetic inhibition and the feasibility of directed-adipogenic differentiation. Acta Biomater. 2014; 10(7):3108–16. [PubMed: 24657674]
54. Fichtner-Feigl S, Strober W, Kawakami K, Puri RK, Kitani A. IL-13 signaling through the IL-13alpha2 receptor is involved in induction of TGF-beta1 production and fibrosis. Nat Med. 2006; 12(1):99–106. [PubMed: 16327802]
55. Kigerl KA, Gensel JC, Ankeny DP, Alexander JK, Donnelly DJ, Popovich PG. Identification of two distinct macrophage subsets with divergent effects causing either neurotoxicity or regeneration in the injured mouse spinal cord. J Neurosci. 2009; 29(43):13435–44. [PubMed: 19864556]
56. Wang Y, Wang YP, Zheng G, Lee VW, Ouyang L, Chang DH, et al. Ex vivo programmed macrophages ameliorate experimental chronic inflammatory renal disease. Kidney Int. 2007; 72(3):290–9. [PubMed: 17440493]
57. Sussman EM, Halpin MC, Muster J, Moon RT, Ratner BD. Porous implants modulate healing and induce shifts in local macrophage polarization in the foreign body reaction. Ann Biomed Eng. 2014; 42(7):1508–16. [PubMed: 24248559]
58. van Putten SM, Ploeger DT, Popa ER, Bank RA. Macrophage phenotypes in the collagen-induced foreign body reaction in rats. Acta Biomater. 2013; 9(5):6502–10. [PubMed: 23376130]
59. Hanson S, D'Souza RN, Hematti P. Biomaterial-mesenchymal stem cell constructs for immunomodulation in composite tissue engineering. Tissue Eng Part A. 2014; 20(15–16):2162–8. [PubMed: 25140989]

60. Pilling D, Vakil V, Cox N, Gomer RH. TNF-alpha-stimulated fibroblasts secrete lumican to promote fibrocyte differentiation. Proc Natl Acad Sci U S A. 2015; 112(38):11929–34. [PubMed: 26351669]

61. Mills CD, Kincaid K, Alt JM, Heilman MJ, Hill AM. M-1/M-2 macrophages and the Th1/Th2 paradigm. J Immunol. 2000; 164(12):6166–73. [PubMed: 10843666]

62. Sans-Fons MG, Yeramian A, Pereira-Lopes S, Santamaria-Babi LF, Modolell M, Lloberas J, et al. Arginine transport is impaired in C57Bl/6 mouse macrophages as a result of a deletion in the promoter of Slc7a2 (CAT2), and susceptibility to Leishmania infection is reduced. J Infect Dis. 2013; 207(11):1684–93. [PubMed: 23460752]

63. Rottensteiner U, Sarker B, Heusinger D, Dafinova D, Rath S, Beier J, et al. In vitro and in vivo Biocompatibility of Alginate Dialdehyde/Gelatin Hydrogels with and without Nanoscaled Bioactive Glass for Bone Tissue Engineering Applications. Materials. 2014; 7(3):1957–74.

64. Xing Q, Yates K, Vogt C, Qian Z, Frost MC, Zhao F. Increasing mechanicalstrength of gelatin hydrogels by divalent metal ion removal. Sci Rep. 2014; 4:4706. [PubMed: 24736500]

65. Migneault I, Dartiguenave C, Bertrand MJ, Waldron KC. Glutaraldehyde: behavior in aqueous solution, reaction with proteins, and application to enzyme crosslinking. Biotechniques. 2004; 37(5):790–6. 8–802. [PubMed: 15560135]

66. Pilipchuk SP, Vaicik MK, Larson JC, Gazyakan E, Cheng MH, Brey EM. Influence of crosslinking on the stiffness and degradation of dermis-derived hydrogels. J Biomed Mater Res A. 2013; 101(10):2883–95. [PubMed: 23505054]

67. Ruhe PQ, Hedberg-Dirk EL, Padron NT, Spauwen PH, Jansen JA, Mikos AG. Porous poly(DL-lactic-co-glycolic acid)/calcium phosphate cement composite for reconstruction of bone defects. Tissue Eng. 2006; 12(4):789–800. [PubMed: 16674292]

68. Bakker D, van Blitterswijk CA, Hesseling SC, Grote JJ. Effect of implantation site on phagocyte/polymer interaction and fibrous capsule formation. Biomaterials. 1988; 9(1):14–23. [PubMed: 2832011]

69. Khanna S, Biswas S, Shang Y, Collard E, Azad A, Kauh C, et al. Macrophage dysfunction impairs resolution of inflammation in the wounds of diabetic mice. PLoS One. 2010; 5(3):e9539. [PubMed: 20209061]

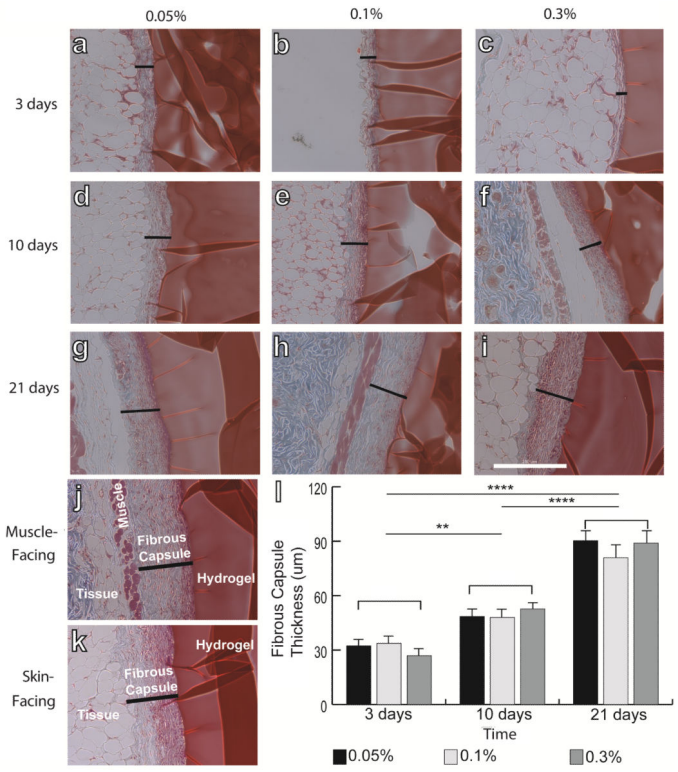

Figure 1.

Masson's trichrome staining of hydrogels explanted after 3 days (a–c), 10 days (d–f), and 21 days (g–i). Hydrogels were crosslinked with glutaraldehyde at concentrations of 0.05% (a, d, g), 0.1% (b, e, h), or 0.3% (c, f, i). Black lines indicate the thickness of the fibrous capsule. (j) Representative image showing the thickness of the fibrous capsule on the muscle-facing (j) and skin-facing (k) sides of the hydrogel. Scale bar is 200um. (l) Thickness of the fibrous capsule, determined from the lengths of the black lines in (a–i). Statistical significance was determined using two way ANOVA and Tukey's post-hoc analysis. No significant differences (n.s.) were observed among different crosslinking concentrations, but differences were found over time. ** denotes $p<0.01$, *** denotes $p<0.005$, **** denotes $p<0.001$.

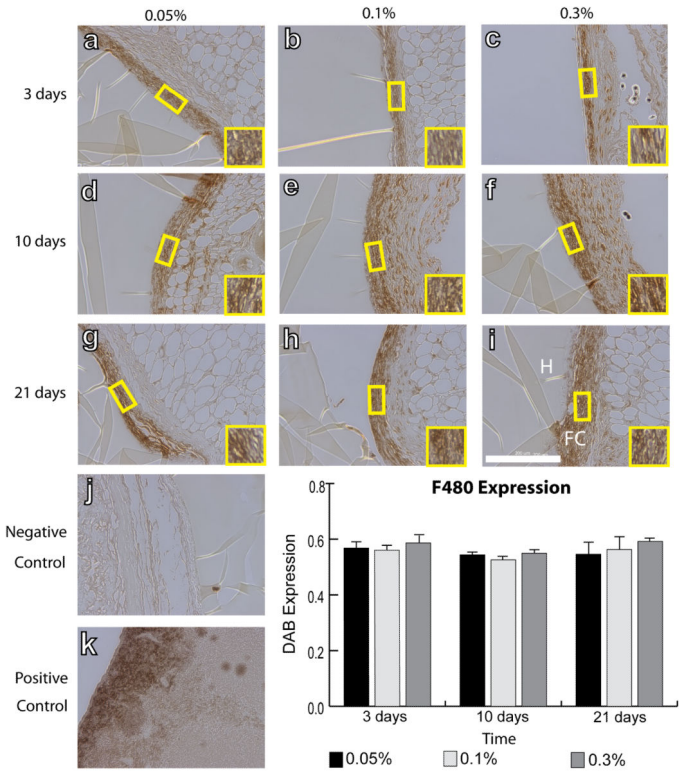

Figure 2.

IHC analysis of F4/80 expression, a pan-macrophage marker, by macrophages surrounding hydrogels explanted after 3 days (a–c), 10 days (d–f), and 21 days (g–i). Hydrogels were crosslinked with glutaraldehyde at concentrations of 0.05% (a, d, g), 0.1% (b, e, h), or 0.3% (c, f, i). (j) Negative control (delete primary) and (k) positive controls (spleen). Scale bar is 200μm. (l) Average staining intensity. Statistical significance was determined using two way ANOVA and Tukey's post-hoc analysis.

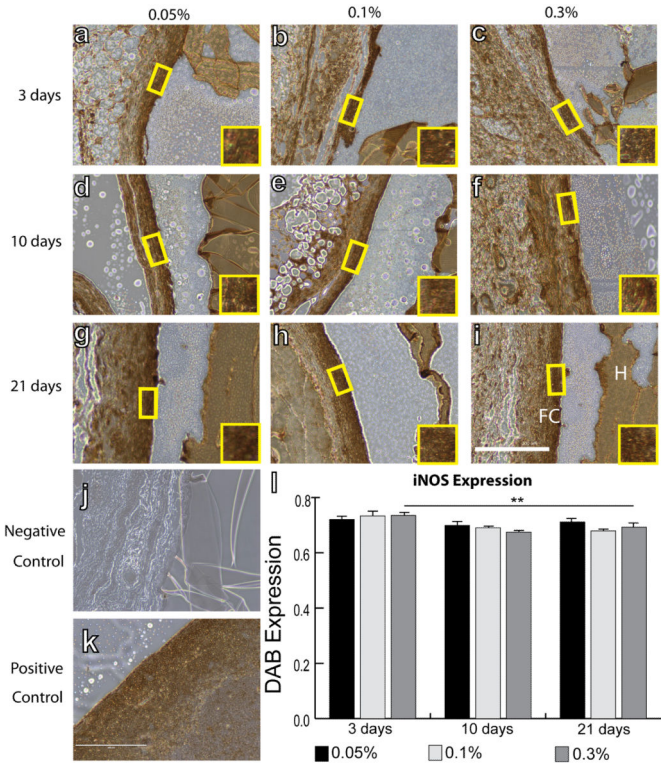

Figure 3.

IHC analysis of iNOS expression, an M1 marker, by macrophages surrounding hydrogels explanted after 3 days (a–c), 10 days (d–f), and 21 days (g–i). Hydrogels were crosslinked with glutaraldehyde at concentrations of 0.05% (a, d, g), 0.1% (b, e, h), or 0.3% (c, f, i). H denotes the hydrogel, while FC denotes the fibrous capsule. Yellow boxes and insets indicate a representative region of intensity quantification. (j) Negative control (delete primary) and (k) positive controls (spleen). Scale bar is 200μm. (l) Average staining intensity. Statistical significance was determined using two way ANOVA and Tukey's post-hoc analysis (**$p<0.01$).

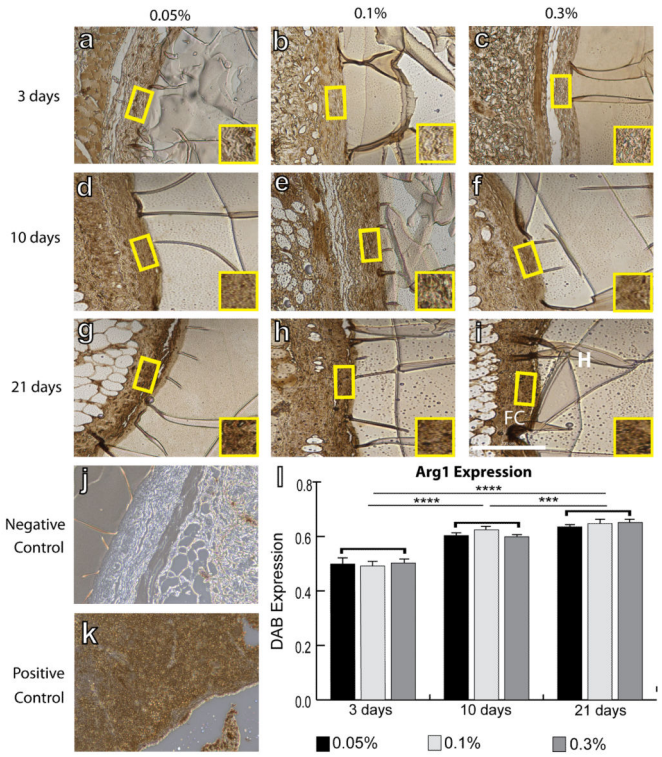

Figure 4.

IHC analysis of Arg1 expression, an M2 marker, by macrophages surrounding hydrogels explanted after 3 days (a–c), 10 days (d–f), and 21 days (g–i). Hydrogels were crosslinked with glutaraldehyde at concentrations of 0.05% (a, d, g), 0.1% (b, e, h), or 0.3% (c, f, i). H denotes the hydrogel, while FC denotes the fibrous capsule. Yellow boxes and insets indicate a representative region of intensity quantification. (j) Negative control (delete primary) and (k) positive controls (spleen). Scale bar is 200μm. (l) Average staining intensity. Statistical significance was determined using two way ANOVA and Tukey's post-hoc analysis (***$p<0.005$, ****$p<0.001$). Note that swelling of the hydrogel in the IHC reagents accounts for its dark staining.

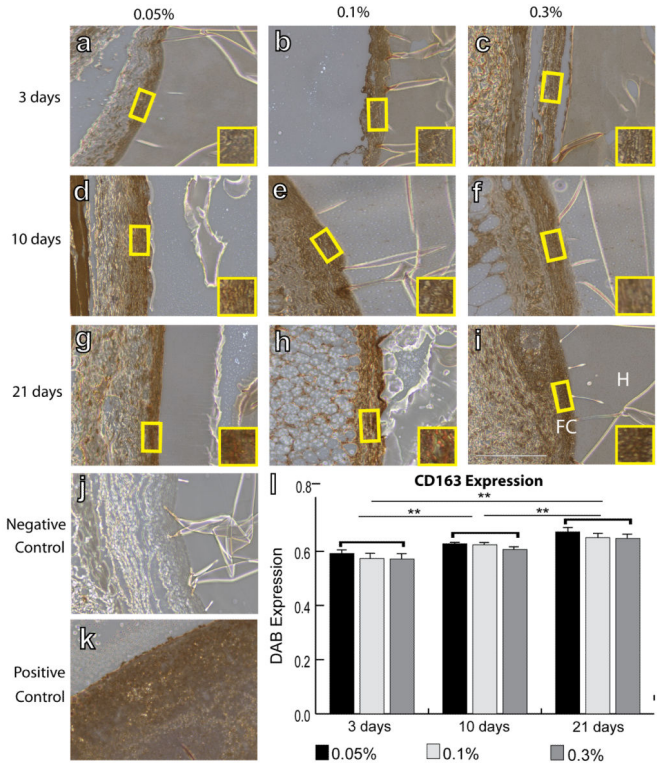

Figure 5.

IHC analysis of CD163 expression, an M2 marker, by macrophages surrounding hydrogels explanted after 3 days (a–c), 10 days (d–f), and 21 days (g–i). Hydrogels were crosslinked with glutaraldehyde at concentrations of 0.05% (a, d, g), 0.1% (b, e, h), or 0.3% (c, f, i). H denotes the hydrogel, while FC denotes the fibrous capsule. Yellow boxes and insets indicate a representative region of intensity quantification. (j) Negative control (delete primary) and (k) positive controls (spleen). Scale bar is 200μm. (l) Average staining intensity. Statistical significance was determined using two way ANOVA and Tukey's post-hoc analysis (**$p<0.01$). Note that swelling of the hydrogel in the IHC reagents accounts for its dark staining.

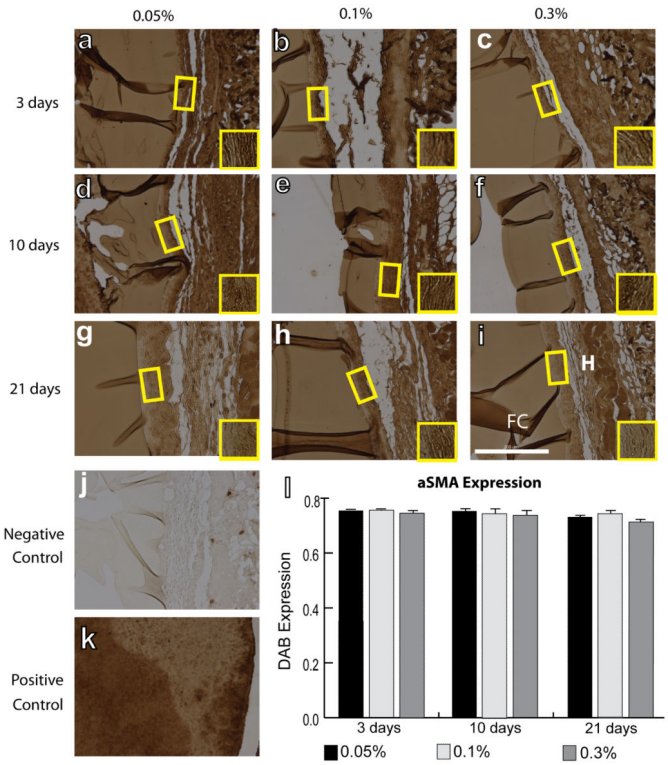

Figure 6.

IHC analysis of α-SMA expression, a myofibroblast marker, on the fibrous capsule of explanted hydrogel after 3 days (a–c), 10 days (d–f), and 21 days (g–i). Hydrogels were crosslinked with glutaraldehyde at concentrations of 0.05% (a, d, g), 0.1% (b, e, h), or 0.3% (c, f, i). H denotes the hydrogel, while FC denotes the fibrous capsule. Yellow boxes and insets indicate a representative region of intensity quantification. (j) Negative control (delete primary) and (k) positive control (spleen). Scale bar is 200 μm. (l) Average staining intensity. Statistical significance was determined using two way ANOVA and Tukey's post-hoc analysis. Note that swelling of the hydrogel in the IHC reagents accounts for its dark staining.

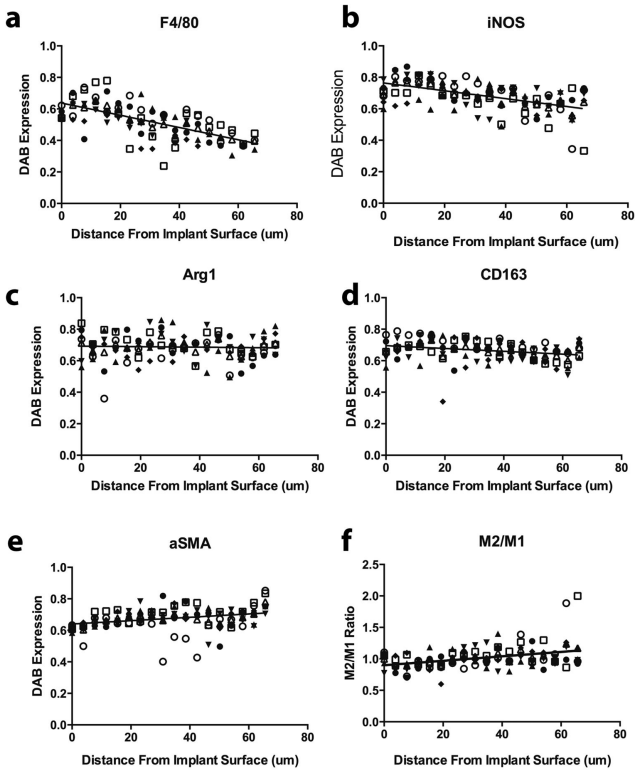

Figure 7.

Spatial distribution of staining intensity of the different markers from inner to the outer edge of the fibrous capsule. Data shown are average values for 0.3% glutaraldehyde at 21 days (n=6), which are representative of trends observed for all hydrogel crosslinking concentrations and time points. Different symbols represent results from different mice.